

Fiber reinforced polymer in civil engineering: Shear lag effect on damaged RC cantilever beams bonded by prestressed plate

Rabahi Abderezak, Tahar Hassaine Daouadji* and Benferhat Rabia

Civil Engineering Department, Laboratory of Geomatics and sustainable development, University of Tiaret, Algeria

(Received December 15, 2020, Revised May 10, 2021, Accepted May 31, 2021)

Abstract. This paper presents a careful theoretical investigation into interfacial stresses in damaged RC cantilever beam with bonded prestressed FRP composites, taking into account loading model, shear lag effect and the prestressed composites impact. These composites are used, in particular, for rehabilitation of structures by stopping the propagation of the cracks. They improve rigidity and resistance, and prolong their lifespan. In this paper, an original model is presented to predict and to determine the stresses concentration at the FRP end, with the new theory analysis approach. This research gives more precision related to the others studies which neglect the effect of prestressed composites coupled with the applied loads. A parametric study has been conducted to investigate the sensitivity of interface behavior to parameters such as laminate and adhesive stiffness, the thickness of the laminate and the fiber orientations where all were found to have a marked effect on the magnitude of maximum shear and normal stress in the composite member. The numerical resolution was finalized by taking into account the physical and geometric properties of materials that may play an important role in reducing the stress values. This research is helpful for the understanding on mechanical behaviour of the interface and design of the FRP-damaged RC hybrid structures.

Keywords: interfacial stresses; prestressed composite; RC cantilever beam; shear lag effect; strengthening

1. Introduction

The rehabilitation or strengthening of reinforced concrete structures is an important problem in civil engineering. In the last few years, FRP composites are being used in the construction industry in the form of laminates and pultruded plates for strengthening of existing structures. Strengthening of an existing structure may become necessary because of a required increase in loading capacity and a change in use, as a result of poor design or construction, or as a consequence of deterioration. In such instances, various techniques may be employed to improve the service ability or ultimate performance of the structure (Smith *et al.* 2002, Tounsi 2006, Hassaine Daouadji *et al.* 2016a, Al-Furjan *et al.* 2020c, Rabahi *et al.* 2018, Rabia *et al.* 2020, Benferhat *et al.* 2021, Al-Furjan *et al.* 2020d, Al-Furjan *et al.* 2021, Benferhat *et al.* 2020, Benhenni *et al.* 2018, Hassaine Daouadji Tahar *et al.* 2019, Bekkaye *et al.* 2020, Bendada *et al.* 2020, Bendenia *et al.* 2020, and Rabahi *et al.* 2019). In recent applications, the use of prestressed laminates has been explored both in laboratory tests

*Corresponding author, Professor, E-mail: daouadjitahar@gmail.com

and in field applications on bridges and other types of structure (Amara *et al.* 2019, Chaded *et al.* 2018, Hassaine Daouadji 2017, Akbaş 2018, Al-Furjan *et al.* 2020b, Guellil *et al.* 2021, Akbaş 2019b, Benhenni *et al.* 2019, Bensattalah *et al.* 2020a, Hassaine Daouadji 2013, Refrafi *et al.* 2020, Tounsi *et al.* 2020, Zine *et al.* 2020, Khatir *et al.* 2019, Kadir *et al.* 2020, Rabahi *et al.* 2020, Rabia *et al.* 2016, Panjehpour *et al.* 2016, Hassaine Daouadji *et al.* 2008, Rabahi *et al.* 2016, Yehia *et al.* 2018, Cheng *et al.* 2019). By prestressing the laminate, the ultra high tensile strength of the composite material can be better utilized, which gives a more effective strengthening scheme. In concrete structures, the compressive stresses induced by prestressing will close existing cracks, reduce crack widths and delay the onset of new cracks in the strengthened structure. Furthermore, the strengthening effect obtained when prestressed FRP laminates are employed will not only be limited to additional imposed loads on the strengthened structure, but will also participate in carrying a portion of the dead load. Analysis of interfacial stresses in beams with bonded plates has been performed by several researchers (Guenaneche *et al.* 2014, Abualnour *et al.* 2019, Akbaş 2019a, Hassaine Daouadji *et al.* 2016a, Liu *et al.* 2019, Pello *et al.* 2020, Bakoura *et al.* 2021, Tounsi *et al.* 2008, Khadimallah *et al.* 2020, Hassaine Daouadji *et al.* 2016b, Kablia *et al.* 2020, Mehran *et al.* 2020, Xue-jun He 2019, Akbaş 2020, Allam *et al.* 2020, Roumaissa *et al.* 2020, Alimirzaei *et al.* 2019, Bensattalah *et al.* 2018, Benferhat *et al.* 2018, Benferhat *et al.* 2019, Bekki *et al.* 2019, Chergui *et al.* 2019, Hamrat *et al.* 2020, Hassaine Daouadji *et al.* 2020, Al-Furjan *et al.* 2020a, Rabia *et al.* 2019, Bensattalah *et al.* 2020b, Tlidji *et al.* 2021, Bekki *et al.* 2021, Benferhat *et al.* 2021, Yu-Hang *et al.* 2020, Rabahi *et al.* 2021, Abdelhak *et al.* 2021).

The problem of interfacial stresses when prestressed laminates are used in strengthening and repair has been treated only by Benachour *et al.* (2008), Rabahi *et al.* (2016). In the first investigation, only interfacial shear stress was studied and the analyzed beam was not loaded, and in the second investigation a rigorous solution for interfacial stresses in simply supported beams strengthened with bonded prestressed FRP plate is developed. In this paper, a theoretical solution and a general model are developed to predict both shear and normal interfacial stress with bonded prestressed FRP laminates and an improved new shear lag and prestressed laminates model are developed for RC damaged cantilever beam strengthened by a prestressed bonded composite plate. The main objective of the present study is to analyze the interfacial stresses in damaged RC cantilever beams strengthened with prestressed FRP plate. The simple approximate closed-form solutions discussed in this paper provide a useful but simple tool for understanding the interfacial behaviour of an externally bonded FRP plate on the damaged concrete cantilever beam with the consideration of the effect of the geometric and mechanical characteristics of the composite plate used as reinforcement.

2. Theoretical approach

2.1 Assumptions of the present solution

Fig. 1 shows the geometry of the damaged RC cantilever beam reinforced with FRP plate composite, and the configuration of the interface of the adhesive layer and the applied load are shown in Fig. 2. The terms V , M , and N present, respectively, the shear force, the bending moment, and the longitudinal tension, while the cantilever beam and the FRP plate are symbolized, respectively, by 1 and 2, $\tau(x)$ and $\sigma_n(x)$ are the shear stress and normal stress, and “ t ” is the component thickness. This analytical and numerical model is made by the following assumptions:

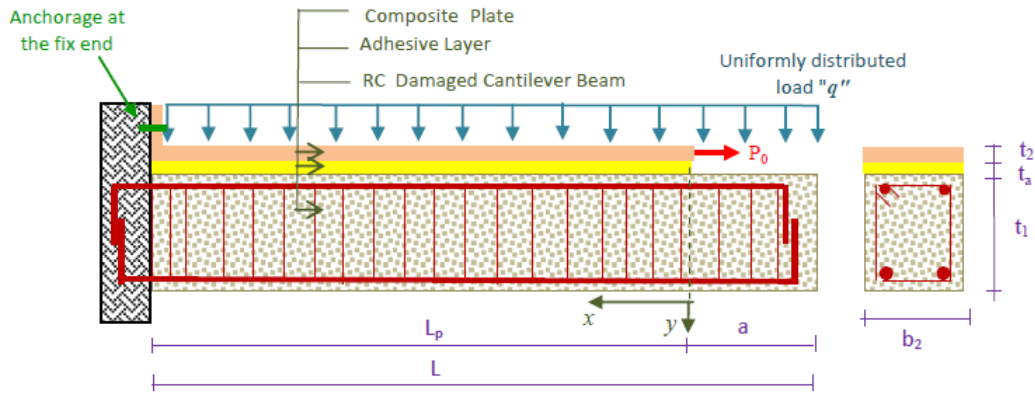


Fig. 1 RC damaged cantilever beam strengthened by a prestressed bonded composite plate

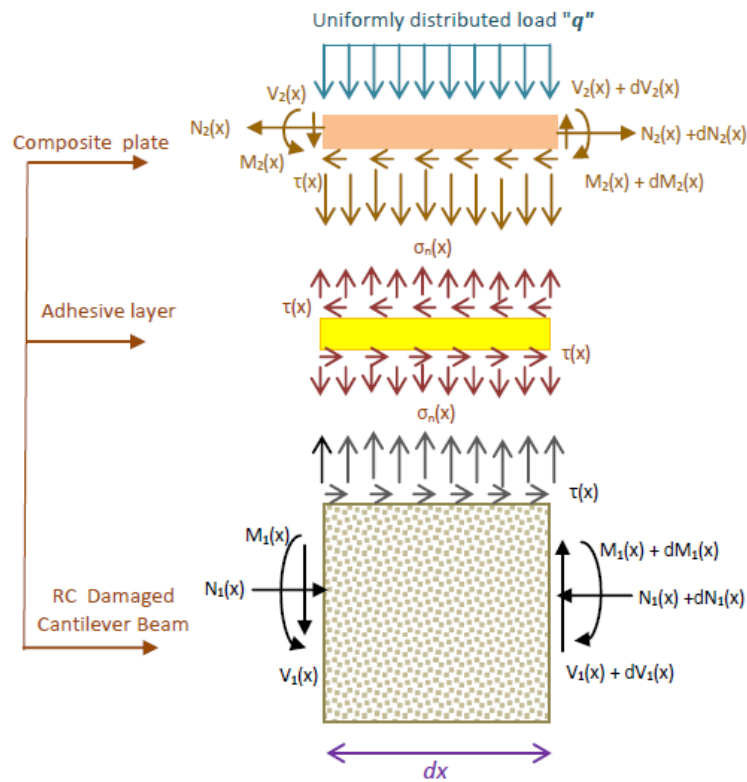


Fig. 2 Forces in differential element of the plated beam

The analytical approach (Hassaine Daouadji *et al.* 2016) is based on the following assumptions:

- Elastic stress strain relationship for FRP and adhesive;
- There is a perfect bond between the FRP plate and the beam;
- The adhesive is assumed to only play a role in transferring the stresses from the FRP beam to the composite plate reinforcement;
- The stresses in the adhesive layer do not change through the direction of the thickness.

2.2 Material properties of damaged concrete beams

The model's Mazars is based on elasticity coupled with isotropic damage and ignores any manifestation of plasticity, as well as the closing of cracks (Mazars *et al.* 1996). This concept directly describes the loss of rigidity and the softening behavior. The constraint is determined by the following expression

$$\sigma_{ij} = (1 - \varphi) E_{ij} \varepsilon_{ij} = \widehat{E}_{ij} \varepsilon_{ij} \quad 0 < d < 1 \quad (1)$$

$$\widehat{E}_{11} = E_{11} (1 - \varphi) \quad \text{long} \quad (2)$$

$$\widehat{E}_{22} = E_{22} (1 - \varphi) \quad \text{trans} \quad (3)$$

where \widehat{E}_{11} , \widehat{E}_{22} and E_{11} , E_{22} are the elastic constants of damaged and undamaged state, respectively. " φ " is damaged variable. Hence, the material properties of the damaged beam can be represented by replacing the above elastic constants with the effective ones defined in Eqs. (2) and (3).

2.3 Distribution forms of the air bubbles in the concrete beam

Because of manufacturing defects in concrete such as the air bubbles " α " that are the subject of the subject, the Young's modulus (E_1) of the imperfect reinforced concrete beam can be written as a functions of thickness coordinate. Several forms of porosity (air bubbles in concrete) have been studied in the present work, which is written in the following forms

$$\check{E}_1 = E_b (1 - \alpha) \quad (4)$$

$$\sigma_{ij} = (1 - \alpha) E_{ij} \varepsilon_{ij} = \check{E}_{ij} \varepsilon_{ij} \quad (5)$$

where \check{E}_1 and E_b is the elastic constants of imperfect and perfect state concrete and α is the index of air bubbles in concrete.

2.4 Adhesive shear stress

The deformation in concrete in the vicinity of the adhesive layer can be expressed by

$$\varepsilon_1(x) = \frac{du_1(x)}{dx} = \frac{y_1}{\check{E}_1 I_1} M_1(x) + \frac{N_1(x)}{\check{E}_1 A_1} + \frac{t_1}{4G_1} \frac{d\tau_a}{dx} \quad (6)$$

Based on the theory of laminated sheets, the deformation of the prestressed laminate composite sheet in the vicinity of the adhesive layer is given by

$$\varepsilon_2(x) = \frac{du_2(x)}{dx} = -D_{11} \frac{t_2}{2b_2} M_2(x) + A_{11} \frac{P_0 + N_2(x)}{b_2} \quad (7)$$

Where $u_1(x)$ and $u_2(x)$ are the horizontal displacements of the concrete beam and the composite plate respectively. $M_1(x)$ and $M_2(x)$ are respectively the bending moments applied to the concrete beam and the composite plate; P_0 is the compression force in the beam due to prestressing, \check{E}_1 is

the Young's modulus of concrete with the taking into account the state of damage and the effect of air bubbles; I_1 the moment of inertia, N_1 and N_2 are the axial forces applied to the concrete and the composite plate respectively, b_2 and t_2 are the width and thickness of the reinforcement plate, $[A']=[A^{-1}]$ is the inverse of the membrane matrix $[A]$, $[D']=[D^{-1}]$ is the inverse of the bending matrix. In what follows, the stiffness of the reinforcement plate is significantly lower than that of the concrete beam to be reinforced. The bending moment in the composite plate can be neglected to simplify the shear stress derivation operations.

The shear stress at the adhesive layer can be expressed as follows

$$\tau_a = \tau(x) = K_s \Delta u(x) = K_s [u_2(x) - u_1(x)] \tag{8}$$

Where K_s is the shear stiffness of the adhesive layer per unit length. From Eq. (8) we can deduce the expression of K_s which is given by

$$K_s = \frac{\tau(x)}{\Delta u(x)} = \frac{\tau(x)}{\Delta u(x)/t_a} \frac{1}{t_a} = \frac{G_a}{t_a} \tag{9}$$

$\Delta u(x)$ is the displacement relative to the adhesive interface, G_a et t_a are the modulus and thickness of the adhesive layer, respectively.

By differentiating the Eqs. (8), (6) and (7) with respect to x , and neglecting the bending moment of the composite plate we will have

$$\frac{d\tau(x)}{dx} = K_s \left[[-D'_{11} \frac{y_2}{b_2} M_2(x) + A'_{11} \frac{P_0 + N_2(x)}{b_2}] - [\frac{y_1}{\tilde{E}_1 I_1} M_1(x) + \frac{N_1}{\tilde{E}_1 A_1} + \frac{t_1}{4G_1}] \right] \tag{10}$$

By differentiating Eq. (10) we will have

$$\frac{d^2\tau(x)}{dx^2} = K_s \left[\frac{A'_{11}}{b_2} \frac{dN_2(x)}{dx} - D'_{11} \frac{t_2}{2b_2} \frac{dM_2(x)}{dx} - \frac{y_1}{\tilde{E}_1 I_1} \frac{dM_1(x)}{dx} + \frac{1}{\tilde{E}_1 A_1} \frac{dN_1(x)}{dx} \right] \tag{11}$$

Substituting $\frac{dM_1(x)}{dx}$, $\frac{dM_2(x)}{dx}$ and $N(x)$ with their following expressions in Eq. (11)

$$N(x) = N_2(x) = N_1(x) = b_2 \int_0^x \tau(x) \tag{12}$$

$$\frac{dM_1(x)}{dx} = \frac{R}{R+1} \left[V_T(x) - b_2 \tau(x) (y_1 + t_a + \frac{t_2}{2}) \right] \tag{13}$$

$$\frac{dM_2(x)}{dx} = \frac{1}{R+1} \left[V_T(x) - b_2 \tau(x) (y_1 + t_a + \frac{t_2}{2}) \right] \tag{14}$$

Allows us to obtain the differential equation of the shear interface stress

$$\frac{d^2\tau(x)}{dx^2} - K_s \left[A'_{11} + \frac{b_2}{\tilde{E}_1 A_1} + \frac{(y_1 + \frac{t_2}{2})(y_1 + t_a + \frac{t_2}{2})}{\tilde{E}_1 I_1 D'_{11} + b_2} b_2 D'_{11} \right] \tau(x) + K_s \left[\frac{(y_1 + \frac{t_2}{2})}{\tilde{E}_1 I_1 D'_{11} + b_2} D'_{11} \right] V_T(x) = 0 \tag{15}$$

The solution to the differential equation (Eq. (15)) above is given by

$$\tau(x) = \gamma_1 \cosh(\eta x) + \gamma_2 \sinh(\eta x) + m_1 V_T(x) \quad (16)$$

With

$$\eta = \sqrt{\frac{A_{11}' + \frac{b_2}{\tilde{E}_1 I_1} + \frac{(2y_1 + t_2)(2y_1 + 2t_a + t_2)}{4\tilde{E}_1 I_1 D_{11}' + b_2} b_2 D_{11}'}{\frac{t_a}{G_a} + \frac{t_1}{4G_1}}} \quad (17)$$

$$m_1 = \frac{1}{2\eta^2} \left(\frac{t_a}{G_a} + \frac{t_1}{4G_1} \right) \left(\frac{(2y_1 + t_2)}{\tilde{E}_1 I_1 D_{11}' + b_2} D_{11}' \right) \quad (18)$$

For our case of a uniformly distributed load, the formula of the shear stress is given by the following equation

$$\tau(x) = \gamma_2 e^{-\alpha x} + m_1 q(a + x) \quad 0 \leq x \leq L_p \quad (19)$$

$$\text{With: } \gamma_2 = \frac{1}{\eta} \left(\frac{t_a}{G_a} + \frac{t_1}{4G_1} \right) \left(\frac{A_{11}'}{b_2} P_0 - \frac{y_1 M_t(0)}{\tilde{E}_1 I_1} \right) - \frac{m_1 q}{\eta} \quad (20)$$

2.5 Adhesive normal stress

The following governing differential equation for the interfacial normal stress (Hassaine Daouadji *et al.* 2016)

$$\frac{d^4 \sigma_n(x)}{dx^4} + \frac{E_a}{t_a} \left(D_{11}' + \frac{b_2}{\tilde{E}_1 I_1} \right) \sigma_n(x) - \frac{E_a}{t_a} \left(D_{11}' \frac{t_2}{2} - \frac{y_1 b_2}{\tilde{E}_1 I_1} \right) \frac{d\tau(x)}{dx} + \frac{q E_a}{\tilde{E}_1 I_1 t_a} = 0 \quad (21)$$

The general solution to this fourth-order differential equation is

$$\sigma_n(x) = e^{-\mu x} [\gamma_3 \cos(\mu x) + \gamma_4 \sin(\mu x)] + e^{\mu x} [\gamma_5 \cos(\mu x) + \gamma_6 \sin(\mu x)] - \zeta_1 \frac{d\tau(x)}{dx} - \frac{q}{D_{11}' \tilde{E}_1 I_1 + b_2} \quad (22)$$

For large values of x it is assumed that the normal stress approaches zero and, as a result, $\gamma_5 = \gamma_6 = 0$. The general solution therefore becomes

$$\sigma_n(x) = e^{-\mu x} [\gamma_3 \cos(\mu x) + \gamma_4 \sin(\mu x)] - \zeta_1 \frac{d\tau(x)}{dx} - \frac{q}{D_{11}' \tilde{E}_1 I_1 + b_2} \quad (23)$$

$$\sigma_n(x) = e^{-\mu x} [\gamma_3 \cos(\mu x) + \gamma_4 \sin(\mu x)] - \frac{2y_1 b_2 - D_{11}' \tilde{E}_1 I_1 t_2}{2D_{11}' \tilde{E}_1 I_1 + b_2} \frac{d\tau(x)}{dx} - \frac{q}{D_{11}' \tilde{E}_1 I_1 + b_2} \quad (24)$$

$$\text{Where: } \mu = \sqrt[4]{\frac{E_a}{4t_a} \left(D_{11}' + \frac{b_2}{\tilde{E}_1 I_1} \right)} \quad (25)$$

As is described by Hassaine Daouadji (2016), the constants γ_3 and γ_4 in Eq. (23) are determined using the appropriate boundary conditions and they are written as follows

$$\gamma_3 = \frac{E_a}{2\mu^3 \tilde{E}_1 I_1 t_a} [V_T(0) + \varpi M_T(0)] - \frac{\zeta_2}{2\mu^3} \tau(0) + \frac{\zeta_1}{2\mu^3} \left(\frac{d^4 \tau(0)}{dx^4} + \mu \frac{d^3 \tau(0)}{dx^3} \right) \quad (26)$$

$$\gamma_4 = -\frac{E_a}{2\mu^2 \tilde{E}_1 I_1 t_a} M_T(0) - \frac{\zeta_1}{2\mu^2} \frac{d^3 \tau(0)}{dx^3} \quad (27)$$

$$\zeta_1 = \frac{2y_1 b_2 - D_{11} \tilde{E}_1 I_1 t_2}{2D_{11} \tilde{E}_1 I_1 + b_2} \quad (28)$$

$$\zeta_2 = \frac{b_2 E_a}{t_a} \left[\frac{y_1}{\tilde{E}_1 I_1} - \frac{D_{11} t_2}{2b_2} \right] \quad (29)$$

The above expressions for the constants γ_3 and γ_4 has been left in terms of the bending moment $M_T(0)$ and shear force $V_T(0)$ at the end of the soffit plate. With the constants B_3 and B_4 determined, the interfacial normal stress can then be found using Eq. (23).

3. Results: Discussion and analysis

3.1 Geometric and material properties

The material used for the present studies is an RC cantilever beam bonded with a glass, carbon and borone fiber reinforced plastic (GFRP, CFRP and BFRP) plate. The cantilever beam is subjected to a uniformly distributed load. A summary of the geometric and material properties is given in Table 1 and Fig. 3. The span of the RC damaged cantilever beam is 1500 mm, the distance from the support to the end of the plate is 500 mm and the uniformly distributed load (UDL) is 30 kN/ml.

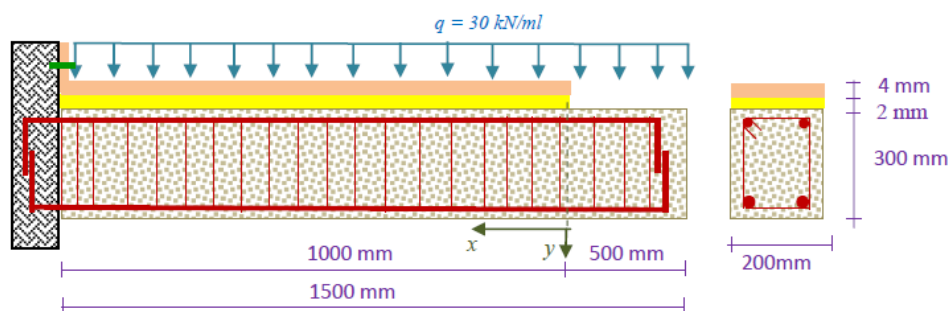


Fig. 3 Geometric characteristics RC damaged cantilever beam strengthening with prestressed composite

Table 1 Geometric and mechanical properties of the materials used

Component	Width (mm)	Depth (mm)	Young's modulus (MPa)	Poisson's ratio
RC beam	$b_1=200$	$t_1=300$	$E_1=30000$	0.18
Adhesive layer	$b_1=100$	$t_a=2$	$E_a=6700$	0.4
Borone fiber	$b_1=100$	$t_2=4$	$E_2=410\ 000$	0.3
HR Carbon fiber	$b_1=100$	$t_2=4$	$E_2=140\ 000$	0.28
E Glass fiber	$b_1=100$	$t_2=4$	$E_2=73\ 000$	0.22
Matrix	--	--	$E_m=3520$	0.34

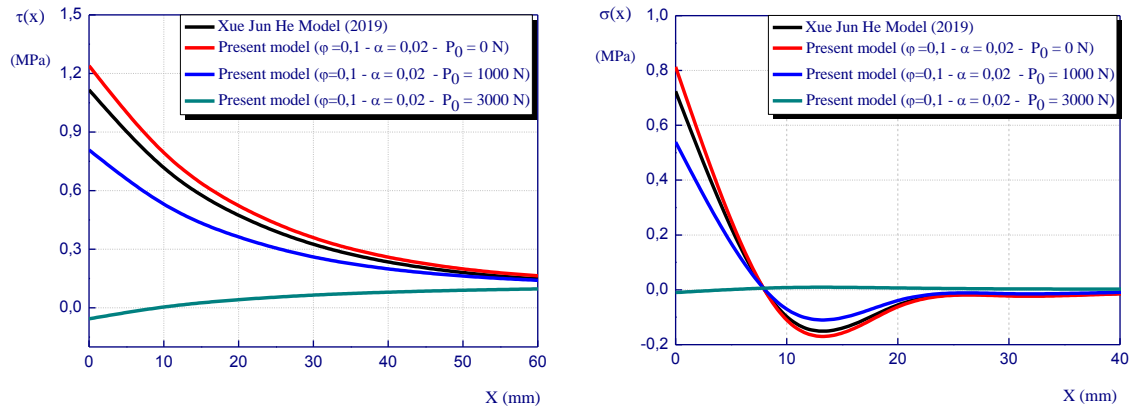


Fig. 4 Variations of interfacial stresses in RC damaged cantilever beam strengthening with prestressed laminate plate: Comparison between the analytical model

3.2 Comparison of analytical solution

To verify the analytical model, the present predictions are compared firstly with to that of the model He (2019) in the case of the absence of the prestressing force ($P_0=0$ kN) and in a second time the current method, by applying a load of the force of prestressing equal to $P_0=1$ kN and $P_0=3$ kN, it is just to see the influence of the prestressing on the interfacial stresses. The width of the laminate was kept constant (200 mm) as well as the laminate length which was chosen to 1000 m leaving a free distance of ($a=500$) leaving a free distance of ($a=500$) between the end of the laminate and the free length of the beam.

Adhesive stresses without prestressing force ($P_0=0$): A comparison of the edge interfacial shear and normal stress from the different closed-form solutions reviewed earlier is undertaken in this section (Fig. 4). An example of a problem is considered, it is a RC damaged cantilever beam strengthening with prestressed laminate plate, the beam is subjected to a uniformly distributed load (UDL) $q=30$ kN/ml. The results of the peak interfacial shear and normal stress (at the end of the soffit plate) are given in Fig. 4. From the presented results, it can be seen that the present solution agree closely with the other methods. Overall, the predictions of the different solutions agree closely with each other. The interfacial normal stress is seen to change sign at a short distance away from the plate end.

3.3 Parametric study

To validate the present analytical solution, the interfacial stresses are calculated and compared with the numerical results, taking into account the effect of some parameters on the distributions of the normal and shear stresses in an damaged RC cantilever beams strengthened by externally bonded with prestressed laminate plate.

3.3.1 Effect of the prestressing force on adhesive stresses

Effect of the prestressing force (P_0) on adhesive stress: In this section, numerical results of the present solution are presented to study the effect of the prestressing force P_0 on the distribution of interfacial stress in RC damaged cantilever beam strengthening with prestressed FRP plate. Three

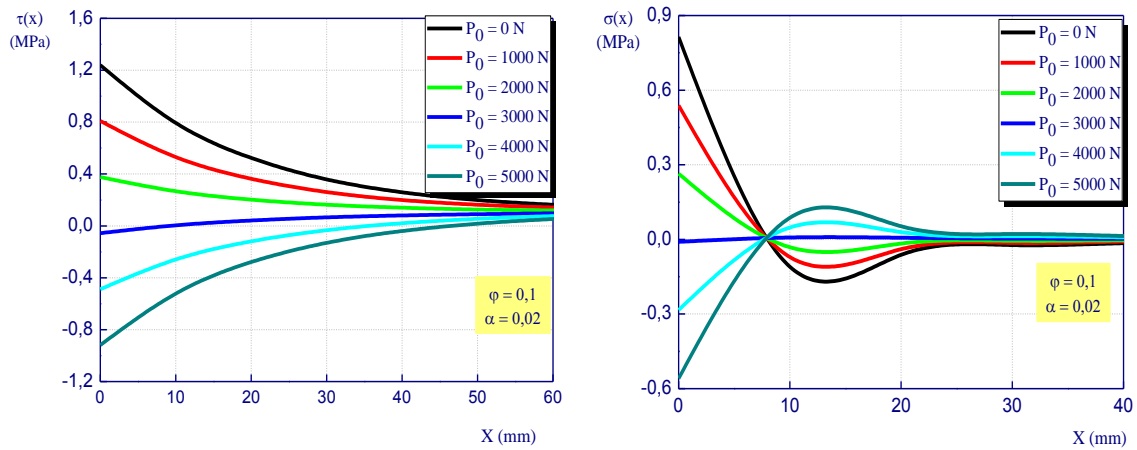


Fig. 5 Adhesive interfacial stresses in RC damaged cantilever beam strengthening with prestressed laminate plate

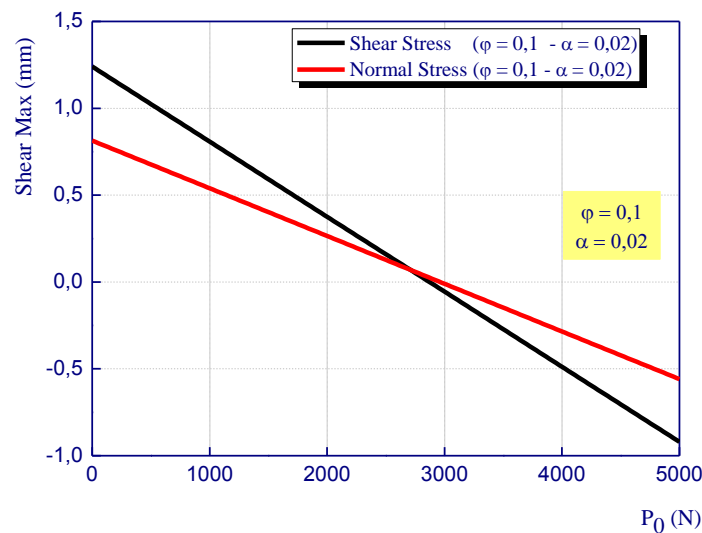


Fig. 6 Effect of prestressing force on interfacial stresses for damaged RC cantilever beam strengthening with prestressed laminate plate

value of P_0 are considered in this study ($P_0=0$ kN; 1 kN, 2 kN, 3 kN, 4 kN and $P_0=5$ kN). Figs. 5 and 6 plot the interfacial shear and normal stress for the RC damaged cantilever beam strengthened with bonded prestressed FRP plate for the uniformly distributed load ($q=30$ kN/ml), From these results, one can observe:

- Maximum stress occur at the ends of adhesively bonded plates, and the normal, or peeling, stress disappears at around 20 mm from the end of the plates.
- It is seen that increasing the value of prestressing force P_0 leads to high stress concentrations.

3.3.2 Effect of plate stiffness

Fig. 7 gives interfacial normal and shear stresses for the damaged RC cantilever beam

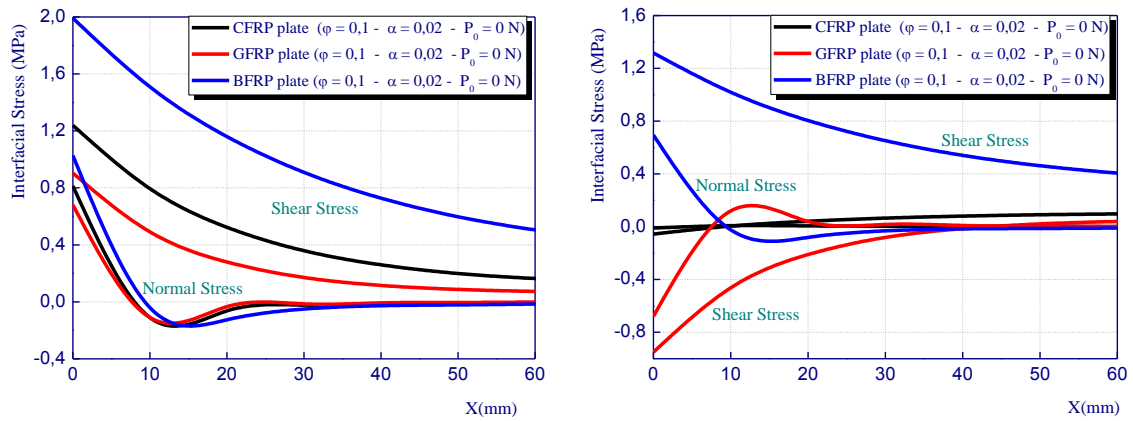


Fig. 7 Effect of plate stiffness on interfacial stresses for damaged RC cantilever beam strengthening with prestressed composite plate

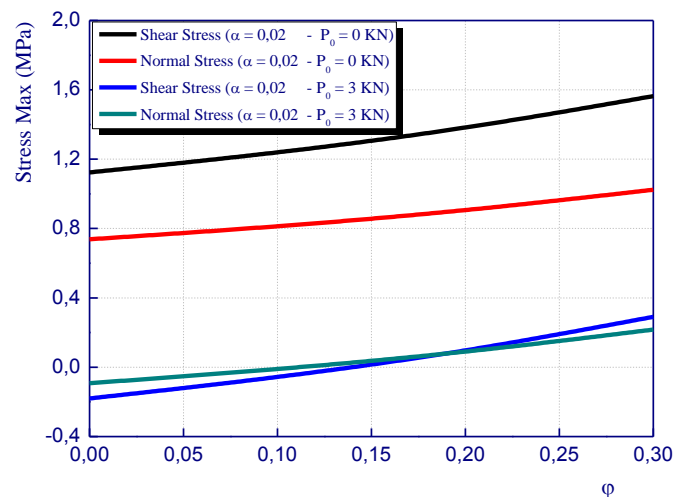


Fig. 8 Effect of damage degree on the maximal interfacial stresses for damaged RC cantilever beam strengthening with prestressed laminate plate

strengthening with prestressed composite plate, in this case: CFRP plate, GFRP plate and BFRP plate, respectively, which demonstrates the effect of plate material properties on interfacial stresses. The length of the plate is $L_p=1000$ mm, and the thickness of the plate and the adhesive layer are both 4mm. The results show that, as the plate material becomes softer (from BFRP to CFRP and then GFRP), the interfacial stresses become smaller, as expected. This is because, under the same load, the tensile force developed in the plate is smaller, which leads to reduced interfacial stresses. The position of the peak interfacial shear stress - moves closer to the free edge as the plate becomes less stiff.

3.3.3 Effect of the damage degree on the maximal interfacial stresses

Fig. 8 illustrates the effect of the different initial damage degrees on the maximum shear and the normal interfacial stresses in damaged RC cantilever beam strengthened with bonded prestressed

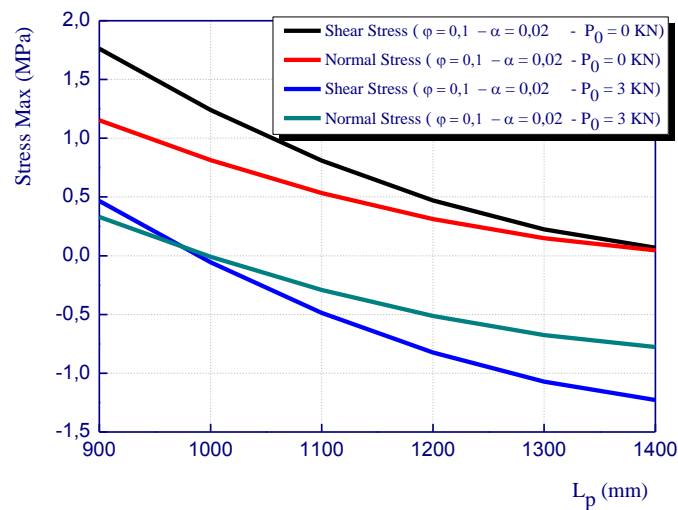


Fig. 9 Effect of plate length of the strengthened beam region L_p on the maximal interfacial stresses for damaged RC cantilever beam strengthening with prestressed laminate plate

laminate plate. It also shows the comparison between the analytical and numerical results for interfacial stresses. According to Fig. 8, it can be observed that both shear and normal stresses decrease slightly with the increase of the initial damage degree (from $d=0$ to 0.3). So, it should be mentioned that these interfacial stresses are very small at $x=25$ mm and 75 mm from the laminate end. In the same context, the results provided in Fig. 8 indicate that the analytical values of the shear stresses are approximately 36% higher than those obtained from the numerical analysis, while the interfacial normal stresses predicted by the numerical results are approximately 19% higher than those calculated by the analytical solution. Fig. 8 show the effect of damage extent on maximum shear and normal interfacial stresses, respectively, for the type of material concerned by this study. The results show that when the damage variable ϕ increases from 0 to 0.3, the maximum interfacial stress increases slowly.

3.3.4 Effect on plate length of the strengthened beam region L_p

Fig. 9 gives the results of the influence of the length of unstrengthened region “ a ” on the interfacial stresses, where “ a ” indicates the length between the end of the composite laminate and the beam support. It is clear from Fig. 9 that, the plate terminates further away from the supports, as the interfacial stresses decrease significantly. Thereby, the interfacial stresses of the beam with 50 mm length, was larger than those of the beam with 200 mm length, as the laminate bonded length of the former was longer than that of the latter. It is noteworthy that the longer bonded length of the composite plate leads to the more ductile failure. For the cantilever beam with the shorter laminate length ($a=200$ mm), the interfacial shear stress distributions were mainly localized within the two end zones of the bond line. Thus, the debonding failure occurred more easily because of the lack of anchorage length (i.e., short bond length of laminate plate). Another interesting observation to be mentioned is when a long composite plate ($a=50$ mm) is used, the interfacial shear stresses are more highly and uniformly distributed along the bond line; thus the magnitude of the interfacial normal stresses are lowered. Therefore, it is recommended to extend as much as possible the strengthening strip to the bond lines.

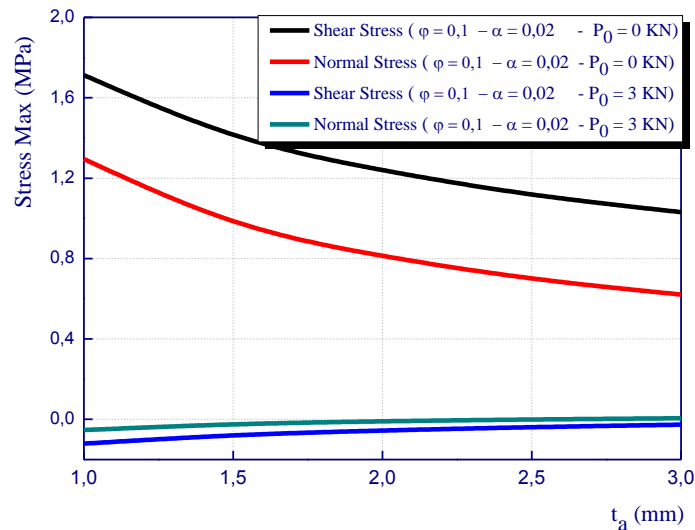


Fig. 10 Effect of the adhesive layer thickness on the maximal interfacial stresses for damaged RC cantilever beam strengthening with prestressed laminate plate

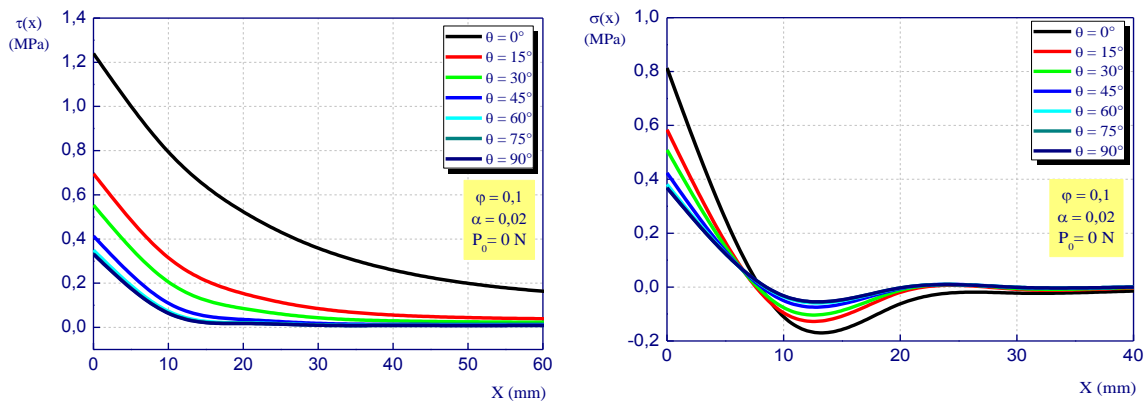


Fig. 11 Effect of various fiber orientations on interfacial stresses for damaged RC cantilever beam strengthening with laminate plate

3.3.5 Effect of the adhesive layer thickness

Fig. 10 show the effects of the adhesive layer thickness and stiffness on the interfacial stresses. It is seen that increasing the adhesive layer thickness leads to significant reduction in the peak interfacial stresses, and the adhesive stiffness to significant increase in the peak interfacial stresses. The maximum adhesive stresses are reached at the plate end region and may be caused premature failure.

3.3.6 Effect of fiber orientation

Fiber orientation is an important variable in the structural design of damaged RC cantilever beam strengthening with laminate plate. In fact, the structural capacity of FRP can be tailored and maximized by aligning fibers along the optimal orientation. For the section studied, various fiber

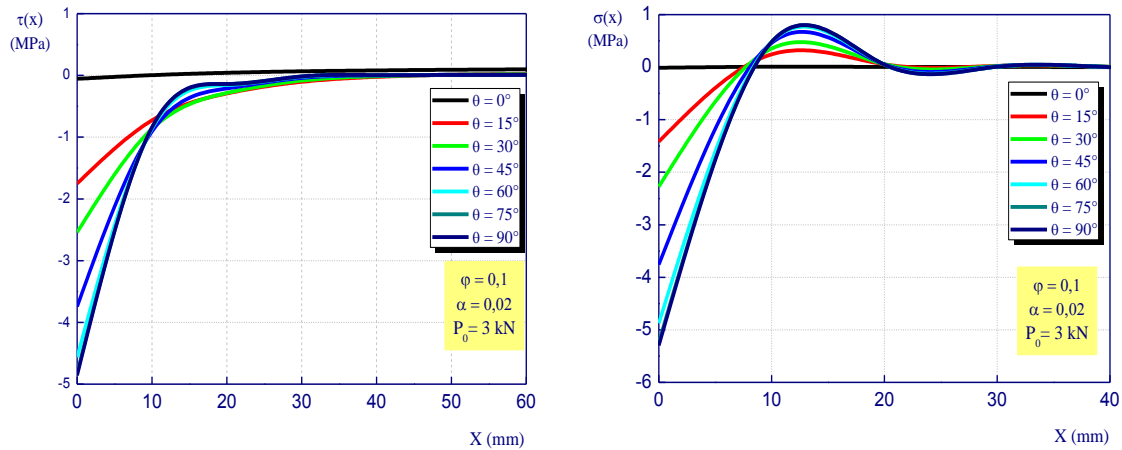


Fig. 12 Effect of various fiber orientations on interfacial stresses for damaged RC cantilever beam strengthening with prestressed laminate plate

orientations were used, notably 0° , 15° , 30° , 45° , 60° , 75° and 90° from the axial (loading) direction. The interfacial stresses for damaged RC beam plotted as function of the fiber orientation are shown in Figs. 11 and 12. It can be seen that when fibers are aligned in beam's longitudinal direction x (0°), it leads to the lowest values of the interfacial stresses, while the fibers are oriented at 90° , the interfacial shear and normal stresses reach the highest values. This is because when fibers are oriented in the beam direction (0°), it provides the highest E -modulus of the plate, which leads to the reduction of the interfacial stresses intensity, as shown in Figs. 11 and 12. Moreover, the shear stress is higher than the transverse normal stress, for fiber with 0° orientation. This difference was found to be relatively small for fibers oriented at 90° from the loading direction.

4. Conclusions

In the present study, a new theoretical interfacial stresses analysis has been presented and conducted has been concerned with the prediction of interfacial shear and normal stresses in damaged RC cantilever beams retrofitted with externally advanced prestressed composite materials. Compared with the existing solutions, the present model is general in nature, and it is applicable to more general loads cases. The results show that there exists a high concentration of shear and peeling stress at the ends of the prestressed laminates. Different fiber arrangements inside the FRP laminate are considered in evaluating the stress mechanism of the strengthened structures. Such interfacial stresses provide the basis for understanding debonding failures in such beams and for development of suitable design rules. Numerical comparison between the existing solutions and the present new solution has been carried out. The damage model is adopted to describe the damage of the RC cantilever beams. The results show that the damage has a significant effect on the interfacial stresses in FRP-damaged RC cantilever beam, especially, when the length of damaged region is equal or superior to the plate length. Consequently, it is recommended to use a strengthening plate having a length that is greater than that of the damaged zone. The results reveal also that the thickness of the FRP strip significantly increases the edge peeling and shear stresses. The parametric study has also shown that in practical applications, where prestressed laminates are to be used for strengthening

structural members, mechanical anchorage devices should be employed in order to avoid premature failure of the strengthening scheme and ensure sufficient anchorage capacity at the ends of the laminates.

Acknowledgments

This research was supported by the Algerian Ministry of Higher Education and Scientific Research (MESRS) as part of the grant for the PRFU research project n° A01L02UN140120200002 and by the University of Tiaret, in Algeria.

References

- Abderezak, R., Daouadji, T.H. and Rabia, B. (2020), "Analysis of interfacial stresses of the reinforced concrete foundation beams repairing with composite materials plate", *Coupl. Syst. Mech.*, **9**(5), 473-498. <http://doi.org/10.12989/csm.2020.9.5.473>.
- Abderezak, R., Daouadji, T.H. and Rabia, B. (2021), "Aluminum beam reinforced by externally bonded composite materials", *Adv. Mater. Res.*, **10**(1), 23-44. <http://doi.org/10.12989/amr.2021.10.1.023>.
- Abderezak, R., Rabia, B., Daouadji, T.H., Abbes, B., Belkacem, A. and Abbes, F. (2019), "Elastic analysis of interfacial stresses in prestressed PFGM-RC hybrid beams", *Adv. Mater. Res.*, **7**(2), 83-103. <https://doi.org/10.12989/amr.2018.7.2.083>.
- Abualnour, M., Chikh, A., Hebali, H., Kaci, A., Tounsi, A., Bousahla, A.A. and Tounsi, A. (2019), "Thermomechanical analysis of antisymmetric laminated reinforced composite plates using a new four variable trigonometric refined plate theory", *Comput. Concrete*, **24**(6), 489-498. <https://doi.org/10.12989/cac.2019.24.6.489>.
- Akbaş, Ş.D. (2018), "Thermal post-buckling analysis of a laminated composite beam", *Struct. Eng. Mech.*, **67**(4), 337-346. <http://doi.org/10.12989/sem.2018.67.4.337>.
- Akbaş, Ş.D. (2019a), "Post-buckling analysis of a fiber reinforced composite beam with crack", *Eng. Fract. Mech.*, **212**, 70-80. <https://doi.org/10.1016/j.engfracmech.2019.03.007>.
- Akbaş, Ş.D. (2019b), "Nonlinear static analysis of laminated composite beams under hygro-thermal effect", *Struct. Eng. Mech.*, **72**(4), 433-441. <http://doi.org/10.12989/sem.2019.72.4.433>.
- Akbaş, Ş.D. (2020), "Dynamic responses of laminated beams under a moving load in thermal environment", *Steel Compos. Struct.*, **35**(6), 729-737. <http://doi.org/10.12989/scs.2020.35.6.729>.
- Al-Furjan, M.S.H., Habibi, M., Chen, G., Safarpour, H., Safarpour, M. and Tounsi, A. (2020b), "Chaotic simulation of the multi-phase reinforced thermo-elastic disk using GDQM", *Eng. Comput.*, 1-24. <https://doi.org/10.1007/s00366-020-01144-2>.
- Al-Furjan, M.S.H., Habibi, M., Ghabussi, A., Safarpour, H., Safarpour, M. and Tounsi, A. (2021), "Non-polynomial framework for stress and strain response of the FG-GPLRC disk using three-dimensional refined higher-order theory", *Eng. Struct.*, **228**, 111496. <https://doi.org/10.1016/j.engstruct.2020.111496>.
- Al-Furjan, M.S.H., Habibi, M., Ni, J., won Jung, D. and Tounsi, A. (2020a), "Frequency simulation of viscoelastic multi-phase reinforced fully symmetric systems", *Eng. Comput.*, 1-17. <https://doi.org/10.1007/s00366-020-01200-x>.
- Al-Furjan, M.S.H., Habibi, M., won Jung, D., Sadeghi, S., Safarpour, H., Tounsi, A. and Chen, G. (2020c), "A computational framework for propagated waves in a sandwich doubly curved nanocomposite panel", *Eng. Comput.*, 1-18. <https://doi.org/10.1007/s00366-020-01130-8>.
- Al-Furjan, M.S.H., Safarpour, H., Habibi, M., Safarpour, M. and Tounsi, A. (2020d), "A comprehensive computational approach for nonlinear thermal instability of the electrically FG-GPLRC disk based on GDQ method", *Eng. Comput.*, 1-18. <https://doi.org/10.1007/s00366-020-01088-7>.

- Ali, Y.A.Z. (2018), "Flexural behavior of FRP strengthened concrete-wood composite beams", *Ain Shams Eng. J.*, **9**(4), 3419-3424. <https://doi.org/10.1016/j.asej.2018.06.003>.
- Alimirzaei, S., Mohammadimehr, M. and Tounsi, A. (2019), "Nonlinear analysis of viscoelastic micro-composite beam with geometrical imperfection using FEM: MSGT electro-magneto-elastic bending, buckling and vibration solutions", *Struct. Eng. Mech.*, **71**(5), 485-502. <https://doi.org/10.12989/sem.2019.71.5.485>.
- Allam, O., Draiche, K., Bousahla, A.A., Bourada, F., Tounsi, A., Benrahou, K.H., ... & Tounsi, A. (2020), "A generalized 4-unknown refined theory for bending and free vibration analysis of laminated composite and sandwich plates and shells", *Comput. Concrete*, **26**(2), 185-201. <http://doi.org/10.12989/cac.2020.26.2.185>.
- Amara, K., Antar, K. and Benyoucef, S. (2019), "Hygrothermal effects on the behavior of reinforced-concrete beams strengthened by bonded composite laminate plates", *Struct. Eng. Mech.*, **69**(3), 327-334. <https://doi.org/10.12989/sem.2019.69.3.327>.
- Bakoura, A., Bourada, F., Bousahla, A.A., Tounsi, A., Benrahou, K.H., Tounsi, A., ... & Mahmoud, S.R. (2021), "Buckling analysis of functionally graded plates using HSDT in conjunction with the stress function method", *Comput. Concrete*, **27**(1), 73-83. <http://doi.org/10.12989/cac.2021.27.1.073>.
- Bekkaye, T.H.L., Fahsi, B., Bousahla, A.A., Bourada, F., Tounsi, A., Benrahou, K.H., ... & Al-Zahrani, M.M. (2020), "Porosity-dependent mechanical behaviors of FG plate using refined trigonometric shear deformation theory", *Comput. Concrete*, **26**(5), 439-450. <http://doi.org/10.12989/cac.2020.26.5.439>.
- Benachour, A., Benyoucef, S., Tounsi, A. and Adda bedia, E.A. (2008), "Interfacial stress analysis of steel beams reinforced with bonded prestressed FRP plate", *Eng. Struct.*, **30**, 3305-15. <https://doi.org/10.1016/j.engstruct.2008.05.007>.
- Bendada, A., Boutchicha, D., Khatir, S., Magagnini, E., Capozucca, R. and Abdel Wahab, M. (2020), "Mechanical characterization of an epoxy panel reinforced by date palm petiole particle", *Steel Compos. Struct.*, **35**(5), 627-634. <http://doi.org/10.12989/scs.2020.35.5.627>.
- Bendenia, N., Zidour, M., Bousahla, A.A., Bourada, F., Tounsi, A., Benrahou, K.H., ... & Tounsi, A. (2020), "Deflections, stresses and free vibration studies of FG-CNT reinforced sandwich plates resting on Pasternak elastic foundation", *Comput. Concrete*, **26**(3), 213-226. <http://doi.org/10.12989/cac.2020.26.3.213>.
- Benferhat, R., Daouadji, T.H. and Abderezak, R. (2021), "Effect of porosity on fundamental frequencies of FGM sandwich plates", *Compos. Mater. Eng.*, **3**(1), 25-40. <http://doi.org/10.12989/cme.2021.3.1.025>.
- Benferhat, R., Daouadji, T.H. and Mansour, M.S. (2016), "Free vibration analysis of FG plates resting on the elastic foundation and based on the neutral surface concept using higher order shear deformation theory", *Comptes Rendus Mecanique*, **344**(9), 631-641. <https://doi.org/10.1016/j.crme.2016.03.002>.
- Benferhat, R., Hassaine Daouadji, T. and Abderezak, R. (2020), "Thermo-mechanical behavior of porous FG plate resting on the Winkler-Pasternak foundation", *Coupl. Syst. Mech.*, **9**(6), 499-519. <http://doi.org/10.12989/csm.2020.9.6.499>.
- Benhenni, M.A., Daouadji, T.H., Abbes, B., Abbes, F., Li, Y. and Adim, B. (2019), "Numerical analysis for free vibration of hybrid laminated composite plates for different boundary conditions", *Struct. Eng. Mech.*, **70**(5), 535-549. <https://doi.org/10.12989/sem.2019.70.5.535>.
- Benhenni, M.A., Daouadji, T.H., Abbes, B., Adim, B., Li, Y. and Abbes, F. (2018), "Dynamic analysis for anti-symmetric cross-ply and angle-ply laminates for simply supported thick hybrid rectangular plates", *Adv. Mater. Res.*, **7**(2), 83-103. <https://doi.org/10.12989/amr.2018.7.2.119>.
- Bensattalah, T., Daouadji, T.H. and Zidour, M. (2020b), "Influences the shape of the floor on the behavior of buildings under seismic effect", *Proceedings of the 4th International Symposium on Materials and Sustainable Development, Vol1-Nano Technology and Advanced Materials*, 26-42. https://doi.org/10.1007/978-3-030-43268-3_3.
- Bensattalah, T., Zidour, M. and Daouadji, T.H. (2018), "Analytical analysis for the forced vibration of CNT surrounding elastic medium including thermal effect using nonlocal Euler-Bernoulli theory", *Adv. Mater. Res.*, **7**(3), 163-174. <https://doi.org/10.12989/amr.2018.7.3.163>.
- Chedad, A., Daouadji, T.H., Abderezak, R., Belkacem, A., Abbes, B., Rabia, B. and Abbes, F. (2018), "A high-order closed-form solution for interfacial stresses in externally sandwich FGM plated RC beams", *Adv. Mater. Res.*, **6**(4), 317-328. <https://doi.org/10.12989/amr.2017.6.4.317>.

- Chergui, S., Daouadji, T.H., Hamrat, M., Boulekbache, B., Bougara, A., Abbas, B. and Amziane, S. (2019), "Interfacial stresses in damaged RC beams strengthened by externally bonded prestressed GFRP laminate plate", *Adv. Mater. Res.*, **8**(3), 197-217. <https://doi.org/10.12989/amr.2019.8.3.197>.
- Daouadji, H.T., Benyoucef, S., Tounsi, A., Benrahou, K.H. and Bedia, A.E. (2008), "Interfacial stresses concentrations in FRP-Damaged RC hybrid beams", *Compos. Interf.*, **15**, 425-440. <https://doi.org/10.1163/156855408784514702>.
- Daouadji, T.H. (2013), "Analytical analysis of the interfacial stress in damaged reinforced concrete beams strengthened by bonded composite plates", *Strength Mater.*, **45**(5), 587-597. <https://doi.org/10.1007/s11223-013-9496-4>.
- Daouadji, T.H. (2017), "Analytical and numerical modeling of interfacial stresses in beams bonded with a thin plate", *Adv. Comput. Des.*, **2**(1), 57-69. <https://doi.org/10.12989/acd.2017.2.1.057>.
- Daouadji, T.H., Chedad, A. and Adim, B. (2016b), "Interfacial stresses in RC beam bonded with a functionally graded material plate", *Struct. Eng. Mech.*, **60**(4), 693-705. <http://doi.org/10.12989/sem.2016.60.4.693>.
- Daouadji, T.H., Rabahi, A., Abbas, B. and Adim, B. (2016a), "Theoretical and finite element studies of interfacial stresses in reinforced concrete beams strengthened by externally FRP laminates plate", *J. Adhes. Sci. Technol.*, **30**(12), 1253-1280. <https://doi.org/10.1080/01694243.2016.1140703>.
- Guellil, M., Saidi, H., Bourada, F., Bousahla, A.A., Tounsi, A., Al-Zahrani, M.M., ... & Mahmoud, S.R. (2021), "Influences of porosity distributions and boundary conditions on mechanical bending response of functionally graded plates resting on Pasternak foundation", *Steel Compos. Struct.*, **38**(1), 1-15. <http://doi.org/10.12989/scs.2021.38.1.001>.
- Guenaneche, B. and Tounsi, A. (2014), "Effect of shear deformation on interfacial stress analysis in plated beams under arbitrary loading", *Adhes. Adhesiv.*, **48**, 1-13. <https://doi.org/10.1016/j.ijadhadh.2013.09.016>.
- Hadj, B., Rabia, B. and Daouadji, T.H. (2019), "Influence of the distribution shape of porosity on the bending FGM new plate model resting on elastic foundations", *Struct. Eng. Mech.*, **72**(1), 823-832. <https://doi.org/10.12989/sem.2019.72.1.061>.
- Hadj, B., Rabia, B. and Daouadji, T.H. (2021), "Vibration analysis of porous FGM plate resting on elastic foundations: Effect of the distribution shape of porosity", *Coupl. Syst. Mech.*, **10**(1), 61-77. <http://doi.org/10.12989/csm.2021.10.1.061>.
- Hamrat, M., Bouziadi, F., Boulekbache, B., Daouadji, T.H., Chergui, S., Labeled, A. and Amziane, S. (2020), "Experimental and numerical investigation on the deflection behavior of pre-cracked and repaired reinforced concrete beams with fiber-reinforced polymer", *Constr. Build. Mater.*, **249**(20), 1-13. <http://doi.org/10.1016/j.conbuildmat.2020.118745>.
- He, X.J., Zhou, C.Y. and Wang, Y. (2019), "Interfacial stresses in reinforced concrete cantilever members strengthened with fibre-reinforced polymer laminates", *Adv. Struct. Eng.*, 1-12. <https://doi.org/10.1177/1369433219868933>.
- Kablia, A., Benferhat, R., Hassaine Daouadji, T. and Bouzidene, A. (2020), "Effect of porosity distribution rate for bending analysis of imperfect FGM plates resting on Winkler-Pasternak foundations under various boundary conditions", *Coupl. Syst. Mech.*, **9**(6), 575-597. <http://doi.org/10.12989/csm.2020.9.6.575>.
- Khadimallah, M.A., Hussain, M., Khedher, K.M., Naeem, M.N. and Tounsi, A. (2020), "Backward and forward rotating of FG ring support cylindrical shells", *Steel Compos. Struct.*, **37**(2), 137-150. <http://doi.org/10.12989/scs.2020.37.2.137>.
- Khatir, S., Tiachacht, S., Thanh, C.L., Bui, T.Q. and Wahab, M.A. (2019), "Damage assessment in composite laminates using ANN-PSO-IGA and Cornwell indicator", *Compos. Struct.*, **230**(15), 111509. <https://doi.org/10.1016/j.compstruct.2019.111509>.
- Liu, S., Zhou, Y., Zheng, Q., Zhou, J., Jin, F. and Fan, H. (2019), "Blast responses of concrete beams reinforced with steel-GFRP composite bars", *Struct.*, **22**, 200-212. <https://doi.org/10.1016/j.istruc.2019.08.010>.
- Mansouri, L., Djebbar, A., Khatir, S. and Wahab, M.A. (2019), "Effect of hygrothermal aging in distilled and saline water on the mechanical behaviour of mixed short fibre/woven composites", *Compos. Struct.*, **207**, 816-825. <https://doi.org/10.1016/j.compstruct.2018.09.067>.
- Mazars, J. and Pijaudier-Cabot, G. (1996), "From damage to fracture mechanics and conversely: A combined approach", *Int. J. Solid. Struct.*, **33**(20), 3327-3342. [https://doi.org/10.1016/0020-7683\(96\)00015-7](https://doi.org/10.1016/0020-7683(96)00015-7).

- Mercan, K., Ebrahimi, F. and Civalek, O. (2020), "Vibration of angle-ply laminated composite circular and annular plates", *Steel Compos. Struct.*, **34**(1), 141-154. <http://doi.org/10.12989/scs.2020.34.1.141>.
- Panjehpour, M., Farzadnia, N., Demirboga, R. and Ali, A.A.A. (2016), "Behavior of high-strength concrete cylinders repaired with CFRP sheets", *J. Civil Eng. Manage.*, **22**(1), 56-64. <https://doi.org/10.3846/13923730.2014.897965>.
- Pello, L., Leire, G., Ignacio, P. and José-Tomás, S.J. (2020), "Flexural strengthening of low-grade reinforced concrete beams with compatible composite material: Steel Reinforced Grout (SRG)", *Constr. Build. Mater.*, **235**, 117790. <https://doi.org/10.1016/j.conbuildmat.2019.117790>.
- Rabahi, A., Daouadji, T.H., Abbes, B. and Adim, B. (2016), "Analytical and numerical solution of the interfacial stress in reinforced-concrete beams reinforced with bonded prestressed composite plate", *J. Reinf. Plast. Compos.*, **35**(3) 258-272. <https://doi.org/10.1177/0731684415613633jrp.sagepub.com>.
- Rabahi, A., Hassaine Daouadji, T., Benferhat, R. and Adim, B. (2018), "Elastic analysis of interfacial stress concentrations in CFRP-RC hybrid beams: Effect of creep and shrinkage", *Adv. Mater. Res.*, **6**(3), 257-278. <https://doi.org/10.12989/amr.2017.6.3.257>.
- Rabia, B., Abderezak, R., Daouadji, T. H., Abbes, B., Belkacem, A. and Abbes, F. (2018), "Analytical analysis of the interfacial shear stress in RC beams strengthened with prestressed exponentially-varying properties plate", *Adv. Mater. Res.*, **7**(1), 29-44. <https://doi.org/10.12989/amr.2018.7.1.029>.
- Rabia, B., Daouadji, T.H. and Abderezak, R. (2019), "Effect of distribution shape of the porosity on the interfacial stresses of the FGM beam strengthened with FRP plate", *Earthq. Struct.*, **16**(5), 601-609. <https://doi.org/10.12989/eas.2019.16.5.601>.
- Rabia, B., Daouadji, T.H. and Abderezak, R. (2019), "Effect of porosity in interfacial stress analysis of perfect FGM beams reinforced with a porous functionally graded materials plate", *Struct. Eng. Mech.*, **72**(3), 293-304. <https://doi.org/10.12989/sem.2019.72.3.293>.
- Rabia, B., Daouadji, T.H. and Abderezak, R. (2020), "Predictions of the maximum plate end stresses of imperfect FRP strengthened RC beams: study and analysis", *Adv. Mater. Res.*, **9**(4), 265-287. <http://doi.org/10.12989/amr.2020.9.4.265>.
- Rabia, B., Daouadji, T.H. and Abderezak, R. (2021), "Effect of air bubbles in concrete on the mechanical behavior of RC beams strengthened in flexion by externally bonded FRP plates under uniformly distributed loading", *Compos. Mater. Eng.*, **3**(1), 41-55. <http://doi.org/10.12989/cme.2021.3.1.041>.
- Refrafi, S., Bousahla, A.A., Bouhadra, A., Menasria, A., Bourada, F., Tounsi, A., ... & Tounsi, A. (2020), "Effects of hygro-thermo-mechanical conditions on the buckling of FG sandwich plates resting on elastic foundations", *Comput. Concrete*, **25**(4), 311-325. <https://doi.org/10.12989/cac.2020.25.4.311>.
- Smith, S.T. and Teng, J.G. (2002), "Interfacial stresses in plated beams", *Eng. Struct.*, **23**(7), 857-871. [http://doi.org/10.1016/S0141-0296\(00\)00090-0](http://doi.org/10.1016/S0141-0296(00)00090-0).
- Tahar, H.D., Abderezak, R. and Rabia, B. (2020), "Flexural performance of wooden beams strengthened by composite plate", *Struct. Monit. Mainten.*, **7**(3), 233-259. <http://doi.org/10.12989/smm.2020.7.3.233>.
- Tahar, H.D., Boussad, A., Abderezak, R., Rabia, B., Fazilay, A. and Belkacem, A. (2019), "Flexural behaviour of steel beams reinforced by carbon fiber reinforced polymer: Experimental and numerical study", *Struct. Eng. Mech.*, **72**(4), 409-419. <https://doi.org/10.12989/sem.2019.72.4.409>.
- Tayeb, B. and Daouadji, T.H. (2020a), "Improved analytical solution for slip and interfacial stress in composite steel-concrete beam bonded with an adhesive", *Adv. Mater. Res.*, **9**(2), 133-153. <https://doi.org/10.12989/amr.2020.9.2.133>.
- Tlidji, Y., Benferhat, R. and Tahar, H.D. (2021), "Study and analysis of the free vibration for FGM microbeam containing various distribution shape of porosity", *Struct. Eng. Mech.*, **77**(2), 217-229. <http://doi.org/10.12989/sem.2021.77.2.217>.
- Tounsi, A. (2006), "Improved theoretical solution for interfacial stresses in concrete beams strengthened with FRP plate", *Int. J. Solid. Struct.*, **43**(14-15), 4154-4174. <https://doi.org/10.1016/j.ijsolstr.2005.03.074>.
- Tounsi, A., Al-Dulaijan, S.U., Al-Osta, M.A., Chikh, A., Al-Zahrani, M.M., Sharif, A. and Tounsi, A. (2020), "A four variable trigonometric integral plate theory for hygro-thermo-mechanical bending analysis of AFG ceramic-metal plates resting on a two-parameter elastic foundation", *Steel Compos. Struct.*, **34**(4), 511-524. <https://doi.org/10.12989/scs.2020.34.4.511>.

- Tounsi, A., Daouadji, T.H. and Benyoucef, S. (2008), "Interfacial stresses in FRP-plated RC beams: Effect of adherend shear deformations", *Int. J. Adhes. Adhesive.*, **29**, 313-351. <https://doi.org/10.1016/j.ijadhadh.2008.06.008>.
- Wang, Y.H., Yu, J., Liu, J.P., Zhou, B.X. and Chen, Y.F. (2020), "Experimental study on assembled monolithic steel-prestressed concrete composite beam in negative moment", *J. Constr. Steel Res.*, **167**, 105667. <https://doi.org/10.1016/j.jcsr.2019.06.004>.
- Yuan, C., Chen, W., Pham, T.M. and Hao, H. (2019), "Effect of aggregate size on bond behaviour between basalt fibre reinforced polymer sheets and concrete", *Compos. Part B: Eng.*, **158**, 459-474. <https://doi.org/10.1016/j.compositesb.2018.09.089>.
- Zenzen, R., Khatir, S., Belaidi, I., Le Thanh, C. and Wahab, M.A. (2020), "A modified transmissibility indicator and Artificial Neural Network for damage identification and quantification in laminated composite structures", *Compos. Struct.*, **248**(15), 112497. <https://doi.org/10.1016/j.compstruct.2020.112497>.
- Zevedejani, M.K. and Beni, Y.T. (2020), "Effect of laminate configuration on the free vibration/buckling of FG Graphene/PMMA composites", *Adv. Nano Res.*, **8**(2), 103-114. <http://doi.org/10.12989/anr.2020.8.2.103>.
- Zine, A., Bousahla, A., Bourada, F., Benrahou, K.H., Tounsi, A., Adda Bedia, E.A., ... & Tounsi, A. (2020), "Bending analysis of functionally graded porous plates via a refined shear deformation theory", *Comput. Concrete*, **26**(1), 63-74. <http://doi.org/10.12989/cac.2020.26.1.063>.
- Zohra, A., Benferhat, R., Tahar, H.D. and Tounsi, A. (2021), "Analysis on the buckling of imperfect functionally graded sandwich plates using new modified power-law formulations", *Struct. Eng. Mech.*, **77**(6), 797-807. <http://doi.org/10.12989/sem.2021.77.6.797>.